

## *Mycobacterium tuberculosis* hijacks host macrophages-derived interleukin 16 to block phagolysosome maturation for enhancing intracellular growth

Haibo Su<sup>a,b,\*</sup>, Shufeng Weng<sup>a,c,\*</sup>, Liulin Luo<sup>d,\*</sup>, Qin Sun<sup>e,\*</sup>, Taiyue Lin<sup>a</sup>, Huixia Ma<sup>a</sup>, Yumo He<sup>a</sup>, Jing Wu<sup>a,c</sup>, Honghai Wang<sup>a</sup>, Wenhong Zhang<sup>a,c</sup> and Ying Xu<sup>a,c</sup>

<sup>a</sup>State Key Laboratory of Genetic Engineering, School of Life Sciences, Department of Infectious Diseases, Shanghai Key Laboratory of Infectious Diseases and Biosafety Emergency Response, National Medical Center for Infectious Diseases, Huashan Hospital, Fudan University, Shanghai, People's Republic of China; <sup>b</sup>Department of Intensive Care Unit, the Second Affiliated Hospital, GMU-GIBH Joint School of Life Science, Guangzhou Medical University, Guangzhou, People's Republic of China; <sup>c</sup>Shanghai Sci-Tech Inno Center for Infection & Immunity, Shanghai, People's Republic of China; <sup>d</sup>Department of Clinical Laboratory, Yangpu Hospital, Tongji University School of Medicine, Shanghai, People's Republic of China; <sup>e</sup>Shanghai Clinical Research Center for Infectious Disease (Tuberculosis), Shanghai Pulmonary Hospital, School of Medicine, Tongji University, Shanghai, People's Republic of China

### ABSTRACT

The discovery of promising cytokines and clarification of their immunological mechanisms in controlling the intracellular fate of *Mycobacterium tuberculosis* (Mtb) are necessary to identify effective diagnostic biomarkers and therapeutic targets. To escape immune clearance, Mtb can manipulate and inhibit the normal host process of phagosome maturation. Phagosome maturation arrest by Mtb involves multiple effectors and much remains unknown about this important aspect of Mtb pathogenesis. In this study, we found that interleukin 16 (IL-16) is elevated in the serum samples of Tuberculosis (TB) patients and can serve as a specific target for treatment TB. There was a significant difference in IL-16 levels among active TB, latent TB infection (LTBI), and non-TB patients. This study first revealed that macrophages are the major source of IL-16 production in response to Mtb infection, and elucidated that IL-16 can promote Mtb intracellular survival by inhibiting phagosome maturation and suppressing the expression of Rev-erba which can inhibit IL-10 secretion. The experiments using zebrafish larvae infected with *M. marinum* and mice challenged with H37Rv demonstrated that reducing IL-16 levels resulted in less severe pathology and improved survival, respectively. In conclusion, this study provided direct evidence that Mtb hijacks the host macrophages-derived interleukin 16 to enhance intracellular growth. It is suggesting the immunosuppressive role of IL-16 during Mtb infection, supporting IL-16 as a promising therapeutic target.


**ARTICLE HISTORY** Received 16 October 2023; Revised 18 February 2024; Accepted 20 February 2024

**KEYWORDS** *Mycobacterium tuberculosis*; phagolysosome conversion; IL-16; macrophages; TB


### Introduction

Tuberculosis (TB) is a global health issue caused by *Mycobacterium tuberculosis* (Mtb) infection [1, 2]. In 2021, approximately 10.6 million individuals were affected by TB, resulting in 1.6 million deaths worldwide and significant social and economic burdens [3, 4]. One of the main factors contributing to such a huge death toll is the limitations of current diagnostic tests and the difficulty of treating tuberculosis, especially when multidrug-resistant tuberculosis is present [5]. In the treatment of Tuberculosis, in addition to the development of new anti-tuberculosis drugs, immunotherapy to enhance the level of host

immune response and attenuate host immune-inflammatory damage is gradually gaining attention [6]. A wide variety of immunological agents are currently available, including vaccines (inactivated bacterial vaccines in combination with chemotherapy or genetic vaccination) [7], cytokines (to enhance the Th1 response and inhibit the Th2 response) [8], non-specific agents (to non-specifically modulate host immune function) and several chemical agents. Although some progress has been made in immunotherapy for TB, immunological agents have a slow clinical onset of action, and some of the drugs are “double-edged swords”, so they should still be treated

**CONTACT** Wenhong Zhang  zhangwenhong@fudan.edu.cn  State Key Laboratory of Genetic Engineering, School of Life Sciences, Department of Infectious Diseases, Shanghai Key Laboratory of Infectious Diseases and Biosafety Emergency Response, National Medical Center for Infectious Diseases, Huashan Hospital, Fudan University, Shanghai 200433, China; Shanghai Sci-Tech Inno Center for Infection & Immunity, Shanghai, 200052, China; Ying Xu  yingxu2520@fudan.edu.cn  State Key Laboratory of Genetic Engineering, School of Life Sciences, Department of Infectious Diseases, Shanghai Key Laboratory of Infectious Diseases and Biosafety Emergency Response, National Medical Center for Infectious Diseases, Huashan Hospital, Fudan University, Shanghai 200433, China; Shanghai Sci-Tech Inno Center for Infection & Immunity, Shanghai, 200052, China People's Republic of China

\*These authors contributed equally to the work.

 Supplemental data for this article can be accessed online at <https://doi.org/10.1080/22221751.2024.2322663>.

© 2024 The Author(s). Published by Informa UK Limited, trading as Taylor & Francis Group, on behalf of Shanghai Shangyixun Cultural Communication Co., Ltd This is an Open Access article distributed under the terms of the Creative Commons Attribution-NonCommercial License (<http://creativecommons.org/licenses/by-nc/4.0/>), which permits unrestricted non-commercial use, distribution, and reproduction in any medium, provided the original work is properly cited. The terms on which this article has been published allow the posting of the Accepted Manuscript in a repository by the author(s) or with their consent.

with caution. Immunological and therapeutic research on tuberculosis has not yet achieved a breakthrough, as the understanding of the pathogenesis of tuberculosis and the mechanisms of protective immunity remains a challenge; the mechanisms of immunotherapy have not yet been clarified, and immunotherapy remains an empirical quest.

Understanding the underlying mechanisms of Mtb is crucial for identifying potential therapeutic targets [9]. When Mtb enters the lungs through the respiratory tract, it is engulfed by alveolar macrophages [10, 11]. Mtb prefers residing in phagosomes, which subsequently fuse with lysosomes to form phagolysosome [12, 13]. This fusion initiates the elimination of Mtb through various pathways, including antigen presentation, apoptosis, and autophagy [14–16]. It is well-established that cytokines play a pivotal role in regulating Mtb survival within macrophages [17]. IFN- $\gamma$ , a cytokine known for conferring microbicidal competence to macrophages, is reported to control Mtb infection and promote its clearance [18]. IFN- $\gamma$  facilitates the conversion of bacterial phagosomes into phagolysosomes, leading to mycobacterial elimination [19]. Conversely, IL-10, an immunosuppressive cytokine, is unable to induce the maturation of mycobacterial phagosomes into phagolysosomes [20, 21]. IL-16 is a multifunctional cytokine that has been associated with various inflammatory conditions and bacterial infection [22]. For instance, IL-16 has been shown to promote *T. whipplei* replication by modulating macrophage activation [23] and contribute to T cell inactivation and excessive inflammation in response to *Staphylococcus aureus* infection [24]. However, the specific role and mechanism of IL-16 in regulating the intracellular fate of Mtb remain largely unknown.

Phagosome maturation is a complex multi-step process and there are multiple Mtb protein and lipid effectors that are thought to play a role in arresting phagosome maturation [25]. However, the specific function(s) of effectors and the interplay between effectors remains to be determined. It also remains unclear if all the effectors of this process are known. The gaps in our understanding are partly due to redundancy among effectors and the potential for effectors to have functions in other aspects of Mtb pathogenesis or physiology beyond phagosome maturation arrest [26, 27]. These features of effectors make it difficult to study the contribution of individual effectors to phagosome maturation arrest using loss of function mutants [28].

In this study, we found that IL-16 was significantly increased in the serum of patients with active tuberculosis compared to patients with LTBI. Mechanistically, IL-16, mainly secreted by macrophages during mycobacterium infection, affects bacilli survival by interfering with the phagolysosome conversion and reversing Rev-erba expression. IL-16 deficiency alleviated bacterial load and attenuated the pathology in *M. marinum*-

infected larvae zebrafish and H37Rv-infected mice. Moreover, neutralizing IL-16 enhanced the pathogen clearance in mice during the early stages of mycobacterial infection, IL-16-deficient mice that also showed tolerance to Mtb. Collectively, these results indicate the immunosuppressive role of IL-16 during Mtb infection, supporting IL-16 as a promising target for treatment TB.

## Results

### **The level of IL-16 is increased in Mtb-infected patients and mice**

To investigate the cytokine involvement in the plasma response of human patients with TB, we categorized the patients into four groups: active TB, treated-TB (3 months post anti-TB chemotherapy), LTBI and healthy donors and assessed the concentrations of 40 host markers in their serum samples using a multiplex cytokine platform. Our findings revealed elevated levels of biomarkers such as IL-10, IL-13, TNF- $\alpha$ , IL-16 and Eotaxin in individuals with active TB, treated-TB and LTBI compared to healthy donors. Notably, we observed a specific increase in IL-16 expression in serum samples from patients with active TB disease when compared to those with treated-TB and LTBI (Figure 1(a)). To validate the findings from chip analysis, enzyme-linked immunosorbent assay (ELISA) was performed to measure the IL-16 level in a larger set of serum samples. The results confirmed that patients with active Mtb infection exhibited a distinct elevation in IL-16 levels in serum samples compared to individuals treated for TB and LTBI (Figure 1(b)). Similarly, mice infected with active Mtb showed a significant increase in IL-16 production in serum samples (Figure 1(c)), BALF samples (Figure 1(d)), and lung homogenates (Figure 1(e)), indicating a significant rise in IL-16 production during active Mtb infection in both humans and mice. We used another cohort to validate the difference in IL-16 secretion and showed significantly higher serum levels of IL-16 in the active TB group (137 TSPOT-positive cases) compared to patients with lung tumours ( $n = 33$ ) and NTM infected patients ( $n = 112$ ) ( $p < 0.01$ ) (Supplementary Fig. 1A). In addition, IL-16 concentration was also effective in differentiating active TB from LTBI patients (31 TSPOT positive cases) (AUC = 0.7526) (Supplementary Fig. 1A and 1B).

### **Macrophages are a major source of IL-16 secretion after mycobacterium infection**

Next, we investigated the induction of IL-16 secretion in mycobacterium-infected macrophages. Analysis of lung cells from mice three weeks after Mtb infection revealed that IL-16-positive cell populations, predominantly macrophages (CD45<sup>+</sup>F4/80<sup>+</sup>), accounted for a significantly higher proportion of cells than T cells

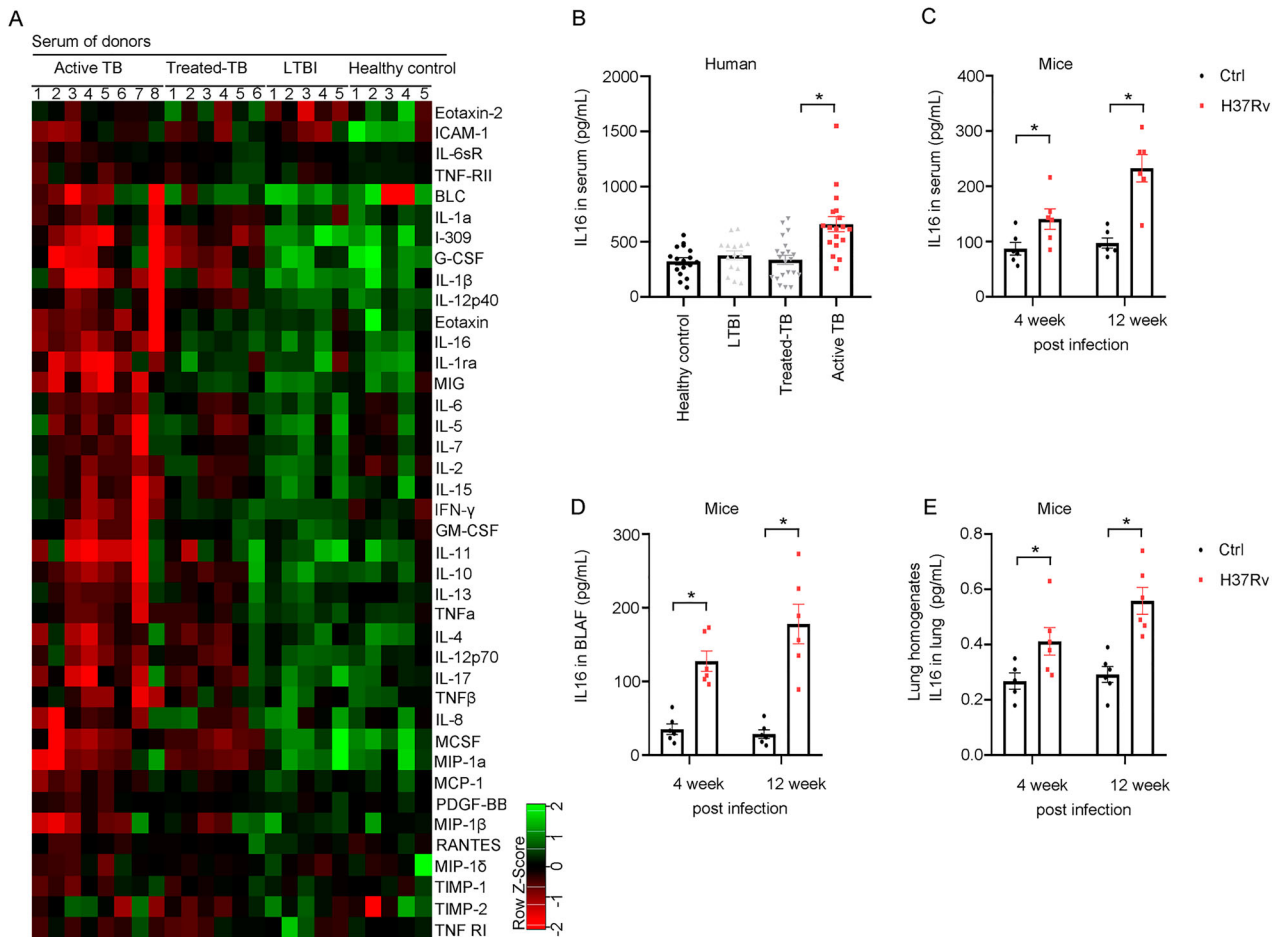


**Figure 1.** The level of IL16 is increased in *Mtb*-infected patients and mice. **A** The concentrations of 40 host markers in serum samples from patients with active TB, treated-TB, LTBI or healthy control using a multiplex cytokine platform ( $n=5$  to  $8$ ). **B** IL16 production by ELISA in serum samples from patients with active TB, treated-TB, LTBI or healthy control ( $n=15$  to  $31$ ). **C** to **E** Six to eight weeks old female C57BL/6 mice were challenged intravenously with  $1 \times 10^6$  CFU of H37Rv. At 4 or 12 weeks after infection, the mice were sacrificed to determine IL-16 level in their serum samples (**C**), Bronchoalveolar lavage fluid (BALF) samples (**D**), and lung homogenates (**E**) ( $n=6$ ). Data represent means  $\pm$  SEM. \* $p < 0.05$ , by 1-way ANOVA/Tukey's multiple comparisons (**B**); Dots show the individual data, \* $p < 0.05$ , by Two-tailed Student's t-test comparing H37Rv and control (**C** and **D**).

(CD3<sup>+</sup>), Neutrophils (CD11b<sup>+</sup>Ly6G<sup>+</sup>), and Dendritic cells (CD24<sup>+</sup>CD103<sup>+</sup>) (Figure 2(a) and Supplementary Fig. 2A). Furthermore, it has also been shown that macrophages derived from human monocytes after *M. marinum* infection have a strong capacity to secrete IL-16 (Supplementary Fig. 2B), and the level of IL-16 increased with higher ratios of bacteria to monocyte-derived macrophages (Figure 2(b)). Macrophages secreting IL-16 were also identified through immunostaining for IL-16 in response to *M. marinum* challenge in THP-1 and RAW 264.7 cells (Figure 2(c) and Supplementary Fig. 2C). Moreover, monocyte-derived macrophages infected with the virulent strain H37Rv, non-virulent strain H37Ra and BCG exhibited increased IL-16 production (Figure 2(d)), whereas a lower level of IL-16 was measured in response to infection with *M. smegmatis* (Figure 2(d)). Notably, we observed a restoration of IL-16 production in monocyte-derived macrophages infected with *M. smegmatis* overexpressing RD1 from *Mtb* (Figure 2(e)).

To investigate the role of macrophages as a primary source of IL-16 production in response to the

mycobacterium challenge *in vivo*, we conducted macrophage depletion experiments using clodronate liposomes administered intravenously (200  $\mu$ L). The following day, the mice were intranasally infected with  $3.0 \times 10^6$  CFU H37Ra in 100  $\mu$ L PBS, followed by another injection of 100  $\mu$ L clodronate liposomes on day 3. On day 6 post-infection, we collected serum and BALF samples from the mice to measure IL-16 levels (Figure 2(f)). Our findings revealed a significant decrease in IL-16 production in both the serum and BALF samples of H37Ra-infected mice (Figure 2(g)), indicating the importance of macrophages as mediators of IL-16 secretion during *Mtb* infection. Notably, H37Ra-infected severe combined immune deficiency (SCID) mice, which lack T and B cells, also exhibited reduced IL-16 levels in BALF compared to wild-type (WT) mice (Supplementary Fig. 2D and 2E). Previously, it has been shown that the TNFR1/caspase-3/8 signaling plays a role in the processing of pro-IL-16 to its active form IL-16. Here, we observed lower levels of IL-16 in *M. marinum*-infected monocyte-derived macrophages in which

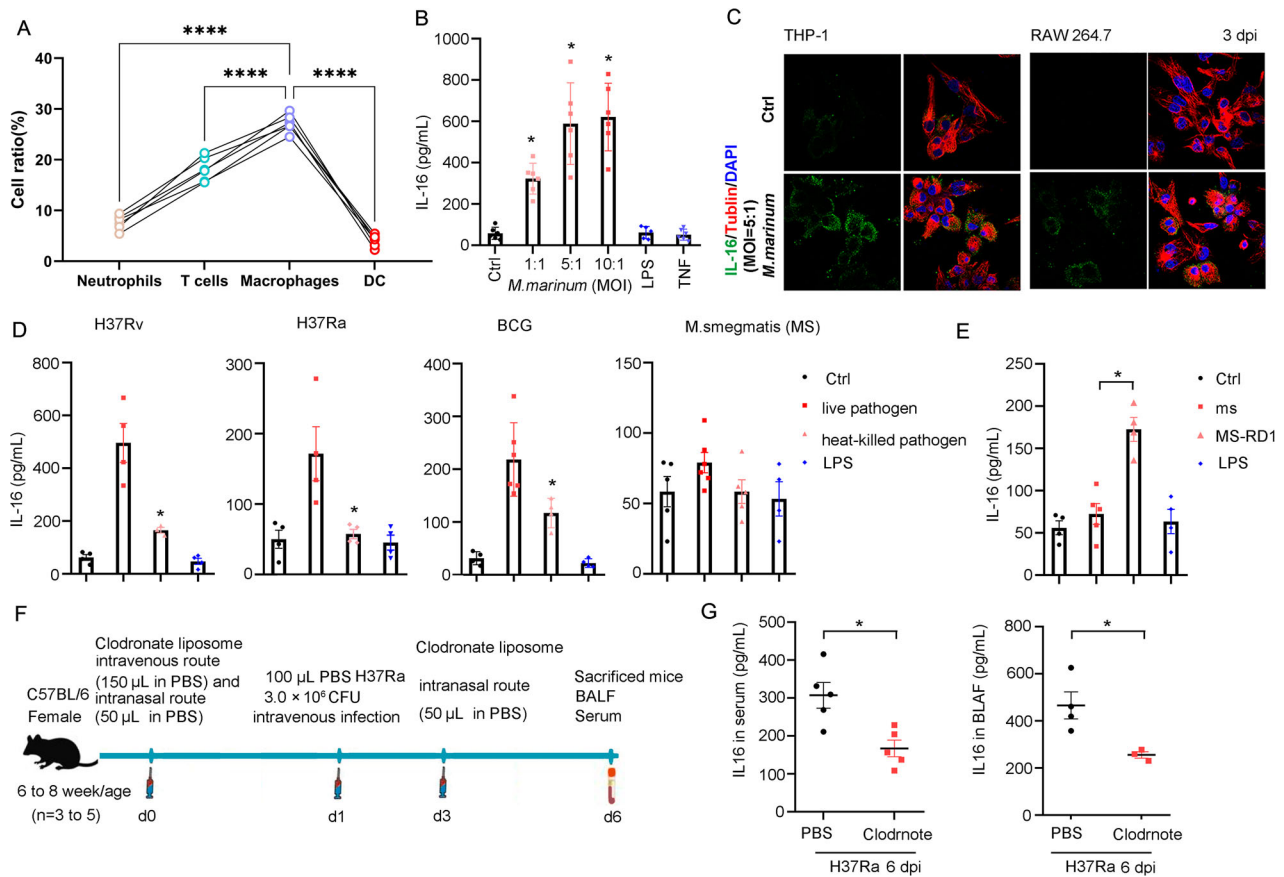


**Figure 2.** Macrophages are a major source of IL-16 secretion after Mycobacterium infection. **A** Analysis of lung cells from mice three weeks after Mtb infection revealed that IL-16-positive cell populations. **B** IL-16 level was increased as the rate of bacteria to monocytes-derived macrophages. Monocyte-derived macrophages were infected with *M. marinum* (MOI = 1:1, 5:1, 10:1) for 4 h. LPS and TNF were added at a concentration of 10 and 100  $\mu$ g/mL, respectively. IL-16 in culture supernatants was quantified by ELISA ( $n = 6$  to 8). **C** Thp-1 and RAW 264.7 were infected with *M. marinum* (MOI = 5:1) for 4 h. Three days post-infection (3 dpi), IL-16 was measured by immunofluorescence using confocal with a 63X oil objective. **D** and **E** Monocytes-derived macrophages were infected with H37Rv, H37Ra, BCG, *M. smegmatis* (MS) or *M. smegmatis* overexpressing RD1 (MS-RD1) at an MOI of 3:1 for 4 h. IL-16 production was measured by ELISA. LPS was added at a concentration of 100  $\mu$ g/mL ( $n = 3$  to 6). **F** Schematic diagram of lung macrophage depletion. Mice aged 6 to 8 weeks were administered clodronate liposomes or PBS control liposomes via the intravenous route (150  $\mu$ L) and the intranasal route (50  $\mu$ L) one day prior to infection. Then, C57BL/6 mice were intravenously challenged with  $3.0 \times 10^6$  CFU of H37Ra in 100  $\mu$ L PBS. Three days post-infection, the mice were injected with clodronate liposomes or PBS control liposomes via the intranasal route (50  $\mu$ L). **G** IL-16 level in BALF and serum 6 days post-infection, according to **f** ( $n = 3$  to 5). data represent means  $\pm$  SEM. \* $p < 0.05$ , by 1-way ANOVA/Tukey's multiple comparisons (**B**, **D**, **E**); Dots show the individual data, \*\* $p < 0.001$ , \*\*\* $p < 0.0001$  by Two-tailed Student's t-test comparing Clodronate and PBS (**G**).

TNFR1 and TLR2 were blocked compared to control cells (Supplementary Fig. 3A). Furthermore, pharmacological inhibition of caspase-3/8 activity decreased IL-16 secretion in monocyte-derived macrophages following *M. marinum* infection, while incomplete attenuation of IL-16 production indicated the involvement of other pathways (Supplementary Fig. 3B). Thus, macrophages are the major source of increased IL-16 after mycobacterium infection.

### IL-16 secretion promotes mycobacterium survival

To investigate the impact of IL-16 on mycobacterium entry, we conducted experiments using alveolar macrophages (AMs) obtained from wild-type (WT) or IL-16 knockout (*Il-16*<sup>-/-</sup>) mice. The AMs were infected with H37Ra at a multiplicity of infection

(MOI) of 5:1 for 4 h, and the uptake of mycobacteria was assessed by counting colony-forming units (CFUs) at 1-hour post-infection (HPI). Surprisingly, we found that the bacterial load in H37Ra-infected *Il-16*<sup>-/-</sup> AMs was comparable to that of WT cells (Figure 3(a)). Additionally, when we neutralized or added IL-16 to macrophages infected with H37Rv (Supplementary Fig. 4A) or *M. marinum* (Supplementary Fig. 4B), we observed no significant difference in bacterial load compared to the control. These findings indicate that IL-16 may not affect the entry-level of mycobacterium in macrophages.

Then, we investigated the potential role of IL-16 in the intracellular survival of mycobacteria. We observed that the bacterial load of H37Rv or *M. marinum* was significantly higher in monocyte-derived macrophages treated with recombinant human IL-16 (rhIL16) compared to control cells

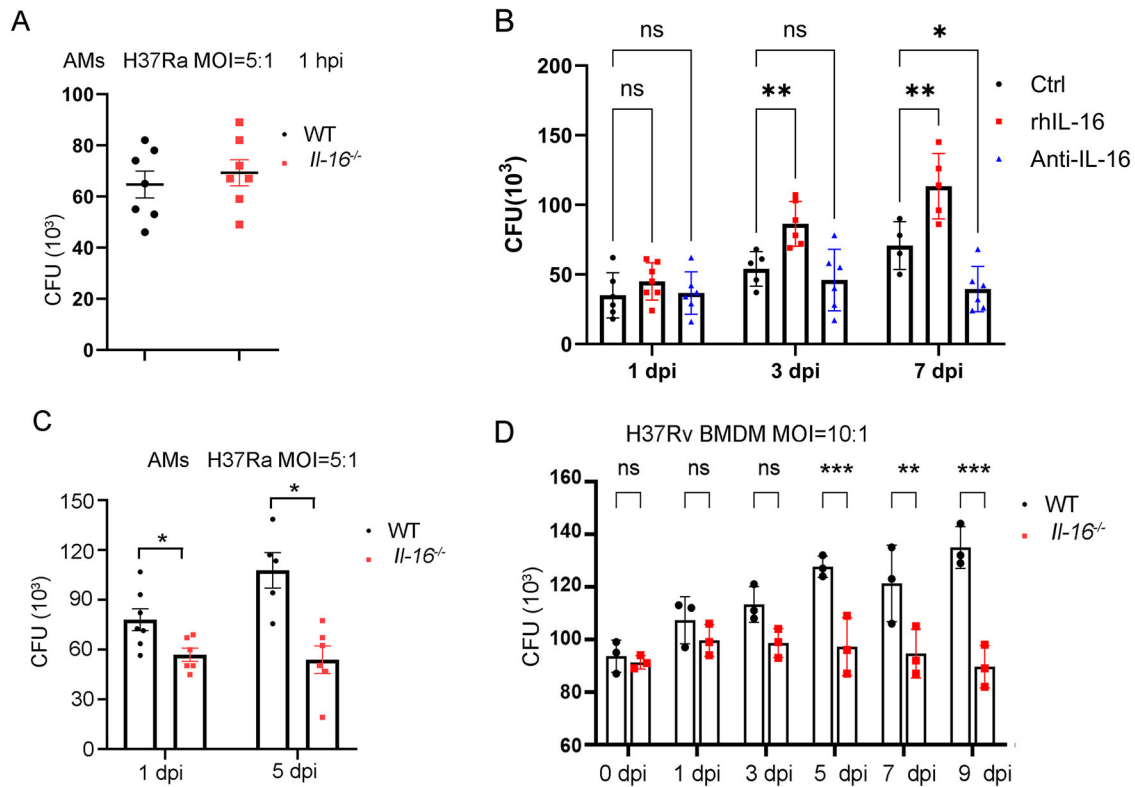


**Figure 3.** IL-16 secretion controls mycobacterium intracellular survival. **A** Alveolar macrophages (AMs) from wild-type (WT) or *Il-16<sup>-/-</sup>* mice were infected H37Ra at an MOI of 5:1 for 4 h. The mycobacterium uptake was measured by CFU counting at 1 hpi ( $n = 7$  to 8). **B** Human monocytes-derived macrophages were pretreated with or without neutralized antibody anti-IL-16 (1  $\mu$ g/mL), rhIL-16 protein (10 ng/mL) for 18 h, infected with H37Rv (MOI = 3:1) for 4 h. Mycobacterium load was measured by CFU counting at 1, 3, and 7 dpi ( $n = 4$  to 7). **C** H37Ra load was measured by CFU counting at 1 and 5 dpi, according to (A) ( $n = 6$  to 8). **D** Bone Marrow-Derived Macrophages (BMDMs) from WT or *Il-16<sup>-/-</sup>* mice were infected H37Rv at an MOI of 3:1 for 4 h. The mycobacterium load was measured by CFU counting at 0 to 9 dpi ( $n = 3$ ). \* $p < 0.05$  compared to media, Student's *t*-test. The graph shown is representative of 2 independent experiments.

(Figure 3(b) and Supplementary Fig. 5). Conversely, when IL-16 was neutralized, the number of bacteria in mycobacterium-infected monocyte-derived macrophages decreased (Fig. 3B and Supplementary Fig. 5). Furthermore, macrophages lacking IL-16 (*Il-16<sup>-/-</sup>*) exhibited lower mycobacterial loads than WT cells following infection with H37Ra and H37Rv (Figure 3(c, d)). These findings suggest that IL-16 promotes the survival of mycobacteria within macrophages.

### IL-16 deficiency promotes macrophage phagosome conversion to clear mycobacteria

To investigate the mechanism of action of IL-16 on the retention of mycobacterium species in macrophages, the process of conversion of mycobacterium phagolysosomes was assessed, we infected macrophages from both WT and *Il-16<sup>-/-</sup>* mice with *M. marinum* (MOI = 10:1) in the presence or absence of recombinant IL-16 protein (10 ng/mL). We observed that IL-16 deficiency led to an enhanced conversion of *M. marinum* phagosomes to phagolysosomes (Figure 4(a,b) and Supplementary Fig. 6). Specifically, at day 2 post-infection, approximately 80% of *M. marinum* phagosomes colocalized with Lamp-1 and cathepsin D in *Il-*

*16<sup>-/-</sup>* macrophages, compared to 50% in WT cells (Figure 4(c)). Furthermore, the addition of exogenous IL-16 protein reversed the increased maturation of *M. marinum* phagosomes in *Il-16<sup>-/-</sup>* macrophages (Figure 4(a-c)). This phenomenon was also observed in macrophages infected with H37Rv, where there was increased co-localization of H37Rv phagosomes with phagolysosomes in *Il-16<sup>-/-</sup>* macrophages compared to WT cells ( $75 \pm 12\%$  vs.  $42 \pm 8\%$ ,  $p < 0.05$ ;  $61 \pm 7\%$  vs.  $18 \pm 4\%$  at 3 dpi,  $p < 0.05$ ) (Figure 4(d,e) and Supplementary Fig. 7). Thus, these findings suggest that the absence of IL-16 rescues the maturation of mycobacterium phagosomes in macrophages. IL-16 is a ligand for CD4, and to investigate whether macrophage-secreted IL-16 affects the maturation of phagocytic lysosomes via the CD4 pathway, we used *Mycobacterium smegmatis* to infect IL-16-deficient BMDM cells and added 10 ng/mL of IL-16 to observe lysosomal transformation. It was found that blocking CD4 and IL-16 with antibodies was more likely to result in the formation of mature lysosomes when IL-16 was added compared to the IgG control (Figure 4(f)). In addition, the PI3K-AKT-mTOR pathway in macrophages inhibits phagolysosome maturation and was significantly inhibited from activation upon IL-16 stimulation with concomitant

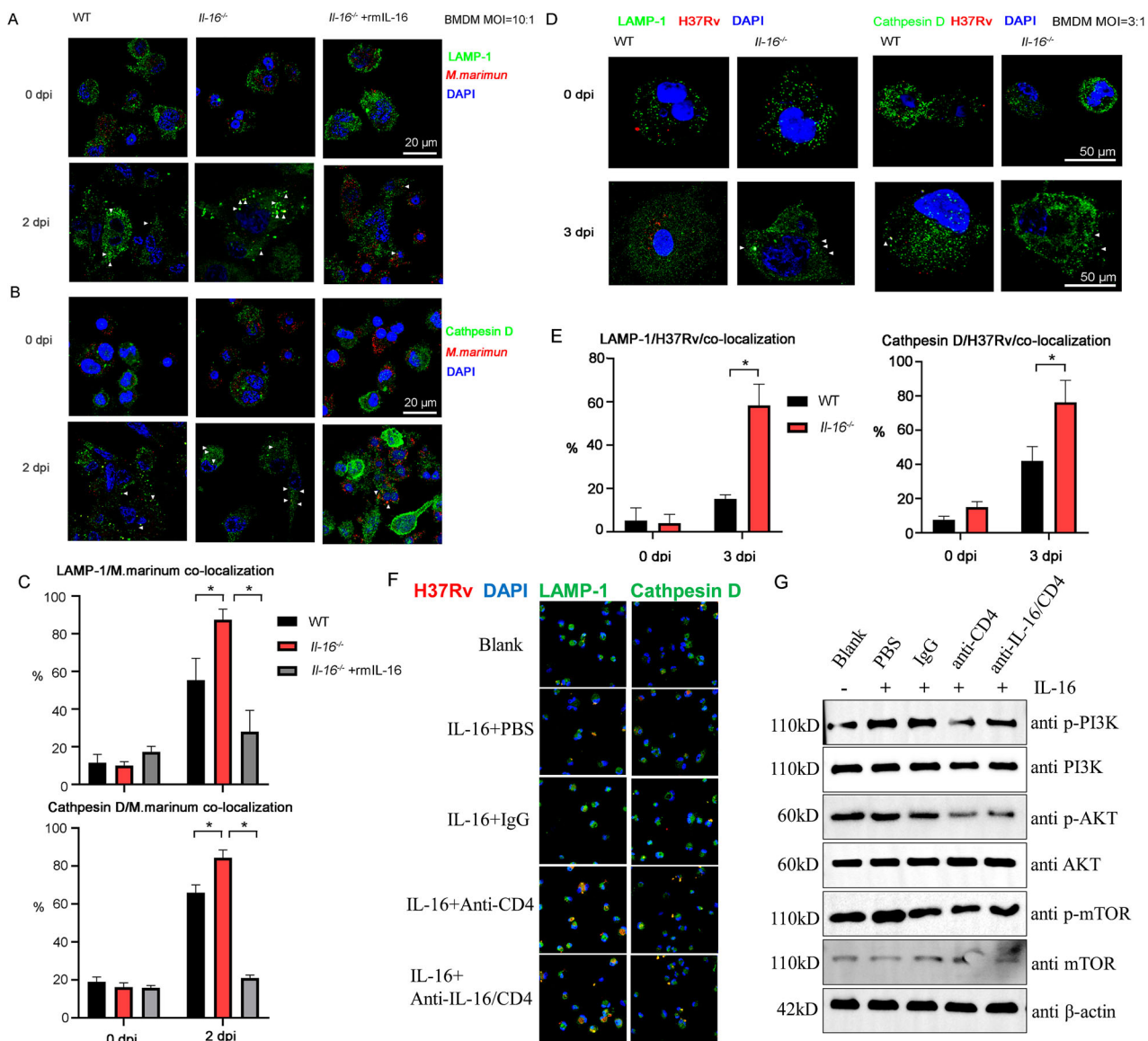


**Figure 4.** IL-16 deficiency promoted phagosome conversion in mycobacterium-infected macrophages. **A** to **B** WT and *Il-16*<sup>-/-</sup> BMDMs were infected with *M. marinum* (MOI = 10:1) in the presence or absence of rmIL-16 protein (10 ng/mL). On day 2 post-infection, Rabbit Abs for *M. marinum*, mouse Abs for Lamp-1 (**A**), and mouse Abs for cathepsin D (**B**) were used. **C** Percent of co-localization of *M. marinum* and Lamp-1 or cathepsin D, according to **A** and **B**. **D** WT and *Il-16*<sup>-/-</sup> BMDMs were infected with H37Rv (MOI = 3:1) in the presence or absence of rmIL-16 protein (10 ng/mL). On day 2 post-infection, Rabbit Abs for H37Rv, mouse Abs for Lamp-1, and mouse Abs for cathepsin D were used. **E** Percent of co-localization of H37Rv and Lamp-1 or cathepsin D, according to **D**. **F** *Il-16*<sup>-/-</sup> BMDMs were infected with H37Rv (MOI = 3:1) in the presence or absence of rmIL-16 protein (10 ng/mL), rabbit anti CD4 or IL-16 and control IgG were added. On day 2 post-infection, Rabbit Abs for H37Rv, mouse Abs for Lamp-1, and mouse Abs for cathepsin D were used. **G** Western blotting analysis was used to examine the activation of PI3 K, AKT, mTOR, according to **F**. \**p* < 0.05 compared to media, Student's *t*-test. The graph shown is representative of 2 independent experiments.

CD4 blockade (Figure 4(g)). The above results suggest that IL-16 inhibits the maturation of phagocytic lysosomes in macrophages through the CD4-activated downstream pathway.

#### Suppression of Rev-erba expression by IL-16 attenuates macrophage response to mycobacterium infection

In *M. marinum*-infected IL-16-deficient BMDM, IL-10 secretion was significantly decreased compared to the WT group (Supplementary Fig. 8), and according to a previous report the level of IL-10 secretion was

strongly associated with Mycobacterium clearance. The adopted orphan nuclear receptor Rev-erba and LXR4 are imperative for transcriptome regulation of IL-10 [29]. Here, we investigated whether IL-16 plays a role in controlling the expression of nuclear receptors, specifically Rev-erba and LXR4, during mycobacterial infection. Macrophages were pretreated with neutralizing anti-IL-16 antibody (1 μg/mL), rhIL-16 protein (10 ng/mL), or left untreated for 18 h. Then, the macrophages were infected with *M. marinum* (MOI = 5:1) for 4 h, washed to remove unphagocytosed bacteria, and incubated for an indicated time with or without blocking antibodies or rhIL-16.

Immunofluorescence staining was used to detect the nuclear expression of Rev-erba and LXR4 at 3 dpi. The results showed that treatment with rhIL-16 inhibited the expression of Rev-erba in *M. marinum*-infected macrophages compared to the control group (Figure 5(a)). Neutralization of IL-16 increased the nuclear recruitment of Rev-erba. However, IL-16 had no effect on the expression of LXR4 or other nuclear receptors (Figure 5(b)). Western blot analysis confirmed the reduced expression of Rev-erba in the presence of rhIL-16 (Figure 5(c)). Moreover, the

protein level of Rev-erba was higher in *Il-16*<sup>-/-</sup> macrophages compared to WT cells (Figure 5(d)).

To investigate the mechanism by which IL-16 inhibits Rev-erba expression, we examined the expression of Pro-IL16, the precursor form of IL-16, in the nucleus of macrophages following *M. marinum* infection (Figure 5(e)). Based on this observation, we hypothesized that Pro-IL16 might repress Rev-erba expression by recruiting a Pro-IL16/GAPBA $\alpha$ /HDAC3 transcriptional inhibition complex, as previously reported to control gene expression [30].

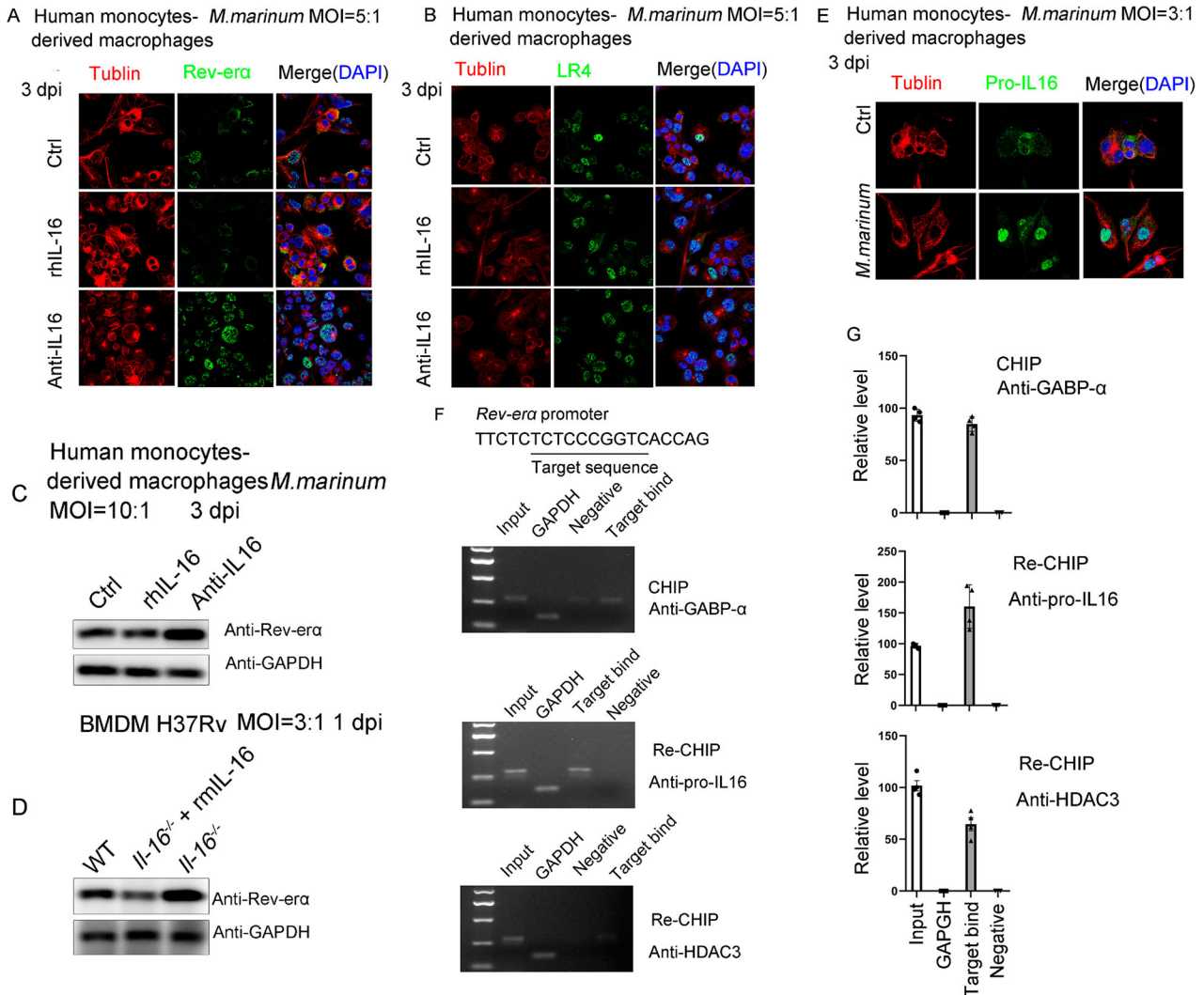


**Figure 5.** IL-16 production repressed Rev-erba expression in macrophages response to mycobacterium challenge. **A** and **B** Monocyte-derived macrophages were pretreated with or without neutralized antibody anti-IL-16 (1  $\mu$ g/mL) or rhIL-16 protein (10 ng/mL) for 18 h. Then, the cells were infected with *M. marinum* (MOI = 5:1) for 4 h. Afterward, the cells were washed to remove unphagocytosed bacteria and further incubated with or without blocking antibodies (1  $\mu$ g/mL) or rhIL-16 (10 ng/mL) for additional time. Immunofluorescence by confocal imaging was used to detect the nuclear expression of Rev-erba (**A**) and LXR4 (**B**) at 3 dpi. **C** Western blotting analysis was used to examine the expression of Rev-erba, according to **A**. **D** WT or *Il-16*<sup>-/-</sup> BMDMs were infected with H37Rv (MOI = 3:1) for 4 h, washed to remove unphagocytosed bacteria and incubated for additional time with or without rhIL-16 (10 ng/mL). Rev-erba protein level was determined by Western blotting at 3 dpi. **E** Immunofluorescence was used to detect the nuclear expression of pro-IL-16 in monocyte-derived macrophages infected with *M. marinum* (MOI = 3:1) at 3 dpi by confocal analysis. **F** A bioinformatic search revealed a putative GAPBA $\alpha$  response motif flanked by a 12 bp sequence of TCTCTCCCGTACC in the *Rev-erba* promoter. Ch-IP, re-ChIP and PCR assay were performed in macrophages infected with *M. marinum* (MOI = 5:1) at 3 dpi. Normal anti-IgG (2  $\mu$ g), anti-pro-IL16 (2  $\mu$ g), anti-GAPBA $\alpha$  (2  $\mu$ g) and anti-HDAC3 (2  $\mu$ g) Abs were used for each immunoprecipitation. PCRs with non-immunoprecipitated genomic DNA (Input) were also performed as control. **G** Relative level of PCR-amplified *Rev-erba* DNA by Image J, according to **F**. \* $p$ <0.05 compared to media, Student's *t*-test. The graph shown is representative of 2 independent experiments.

Bioinformatic analysis revealed a putative half-site motif flanked by a 12 bp TCTCTCCCGGTC sequence, suggesting a GAPBA $\alpha$  response element in the Rev-erba promoter (Figure 5(f)). To determine whether GAPBA $\alpha$  binds to the Rev-erba promoter, we performed ChIP using anti-GAPBA $\alpha$  antibodies and PCR assays in *M. marinum*-infected macrophages. Our results demonstrated direct and equivalent binding of GAPBA $\alpha$  to the proximal Rev-erba promoter (Figure 5(f,g)). Re-ChIP and reporter assay data supported that the Pro-IL16/GAPBA $\alpha$ /HDAC3 complex induced by *M. marinum* infection negatively regulates Rev-erba transcription (Figure 5(f,g)). Consequently, mycobacterium infection leads to the translocation

of Pro-IL16 into the nucleus, where it recruits GAPBA $\alpha$  and HDAC3 to repress Rev-erba expression.

### The IL-16 morphant zebrafish larvae had less-severe pathology and longer survival after *M. marinum* infection

To determine the role of IL-16 in mycobacterial infection, *M. marinum*-infected zebrafish larvae are used as a model system to study the pathogenesis (Figure 6 (a)). Briefly, the morpholino oligos of precursor IL-16 was designed against the translational splice site between the 2 exons and intron to completely abolish IL-16 signaling, including any that may occur via the

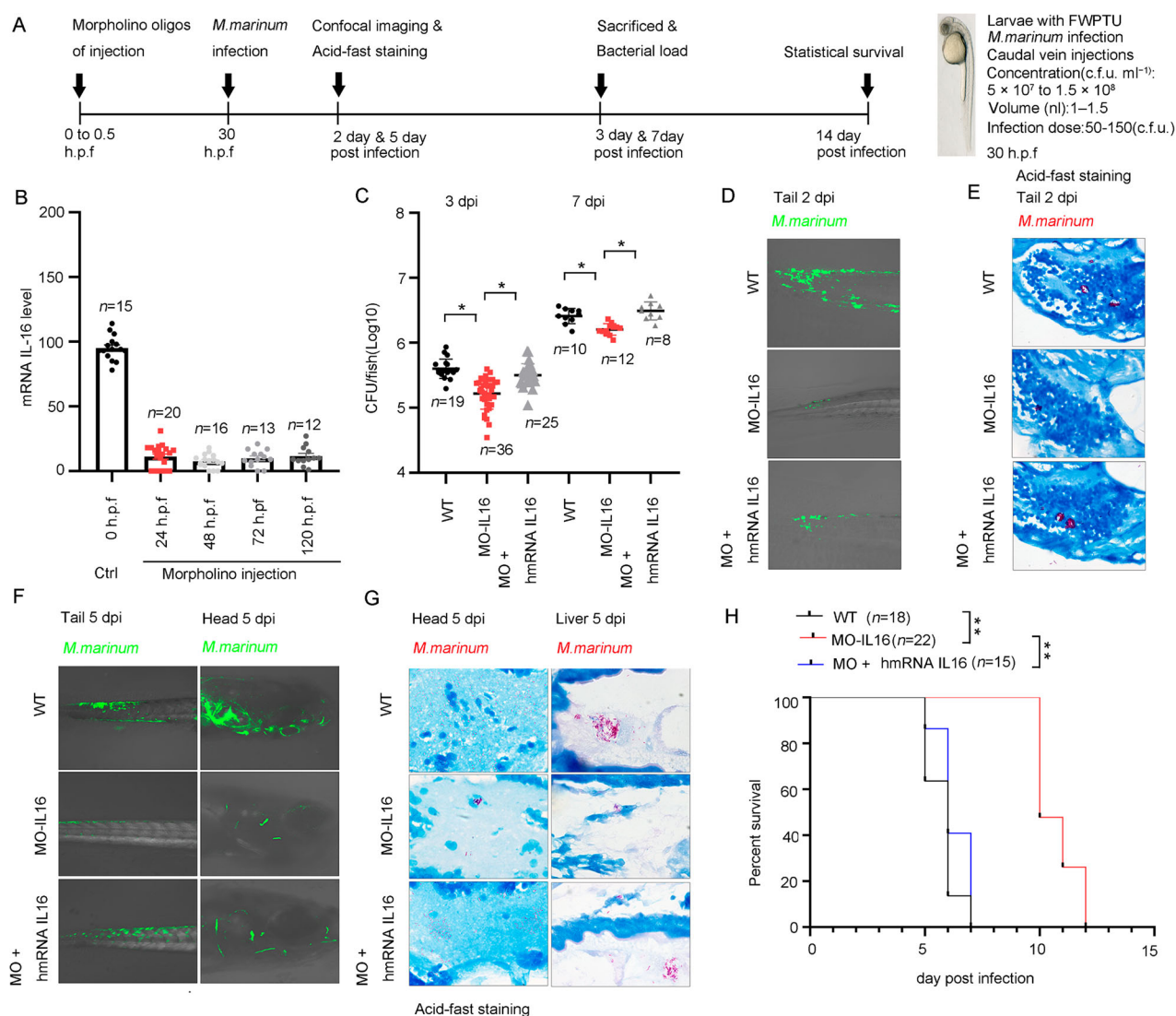


**Figure 6.** IL-16 impaired the clearance of *M. marinum* in zebrafish larvae. **A** Timeline of animal vaccination, infection and killing. Zebrafish larvae were injected with morpholino (MO)-IL-16 (10 ng), MO-control (10 ng), MO-IL-16 (10 ng) plus human IL-16 mRNA (100 pg) at 0–0.5 h.p.f. Zebrafish infection with *M. marinum* was performed via caudal vein injection with 1.0 to 1.5 nl per fish of a single-cell bacterial suspension in PBS at a dosage of  $5.0 \times 10^7$  CFU/mL at 30 h.p.f. **B** The relative level of IL-16 mRNA by qPCR in zebrafish larvae injected with morpholino oligos at indicated time ( $n = 12$  to 20). **C** To assess the bacterial burdens, the homogenates of fish livers were plated onto 7H10 agar by serial dilution to determine CFU at 3 and 7 dpi ( $n = 8$  to 36). **D** and **F** The overall reduction of infection level was determined by fluorescence microscopy. **E** and **G** Ziehl-Neelsen acid-fast staining was performed on 5  $\mu$ m sections for gross pathology. **H** The survival of zebrafish during a 14-day infection. data represent means  $\pm$  SEM. \* $p < 0.05$ , by 1-way ANOVA/Tukey's multiple comparisons (**B**, **C**); A pool of 2 experiments is shown, including 15 to 22 zebrafish larvae per group as indicated, \*\* $p < 0.01$  by log-rank test (**H**).



alternate IL-16 gene in the zebrafish genome. The morpholino oligos or a combination of morpholino oligos and hmRNA IL-16 were microinjected into single-to-two-cell stage zebrafish embryos, which were then infected with *M. marinum* at 30 h post-fertilization (h.p.f.) via caudal vein injections. Our results demonstrated that injection of morpholinos into fertilized eggs effectively abolished IL-16 mRNA expression from 1 to 5 days post-fertilization (d.p.f.) (Figure 6(b)). Furthermore, the *M. marinum* load in IL-16 morphant larvae was significantly reduced at 3- and 7-days post-infection (dpi) (Figure 6(c)). Conversely, the combination of morpholino oligos and hmRNA IL-16 in zebrafish larvae reversed the reduction in bacterial load (Figure 6(c)). Fluorescence imaging revealed a marked decrease in infection levels at 2 and 5 dpi in larvae treated with IL-16 morpholino oligos (Figure 6(d,f)). In IL-16 morphant larvae, well-organized granulomas with bacteria inside were observed, limited tissue damage was detected, and there was less dissemination of bacterial cells (Figure 6(e,g)). Additionally, the survival rate of IL-16 morphant larvae significantly increased compared to control larvae and IL-16 hmRNA-rescued larvae (Figure 6(h)). Collectively, these findings indicate that inhibition of IL-16 is crucial for the early-stage clearance of mycobacterial infection.

### **Interleukin 16 deficiency reduced the host susceptibility to *Mycobacterium tuberculosis* infection**

To investigate the role of IL-16 in mediating the detrimental effects of *Mycobacterium tuberculosis* infection, WT, and *Il-16*<sup>-/-</sup> mice were aerosol-infected with approximately 200 CFU of the H37Rv strain. The bacterial burden and pulmonary pathology were examined at 3, 7 or 28 dpi (Figure 7(a)). Our findings revealed a substantial decrease in H37Rv lung and spleen burden in *Il-16*<sup>-/-</sup> mice compared to WT mice, both early (7 dpi) and late (28 dpi) following infection (Figure 7(b)). However, there was no significant difference in H37Rv lung burden between WT and *Il-16*<sup>-/-</sup> mice at 3 dpi (Figure 7(b)). Moreover, histological examination using H&E staining showed alveolar damage and infiltrating immune cells in the lungs of H37Rv-infected WT mice. In contrast, age-matched H37Rv-infected *Il-16*<sup>-/-</sup> mice exhibited lower inflammation and less necrosis at 7 or 28 dpi (Figure 7(c,d)). Specifically, H-Score analysis demonstrated high expression and localization of Lamp-1 and cathepsin D within the lungs of H37Rv-infected *Il-16*<sup>-/-</sup> mice compared to WT mice at 7 or 28 dpi (Figure 7(e,f)). These results indicate that early and sustained IL-16 production contributes to severe disease progression and significantly increases H37Rv burden.

### **Neutralizing IL-16 molecule could be used to treat tuberculosis infections**

Mycobacterium infection leads to the translocation of Pro-IL16 into the nucleus, where it recruits GAPBaa and HDAC3 to repress Rev-erba expression<sup>[7]</sup>secreted IL-16 activated the PI3K-AKT-mTOR pathway via CD4 and inhibited the maturation of phagolysosomes, allowing better survival of the mycobacterium (Figure 8(a)). To further investigate the potential of blocking endogenous IL-16 to reduce mycobacterium survival in vivo, we performed experiments in SCID mice. Two hours before infection, the mice were intraperitoneally injected with a neutralizing anti-IL-16 antibody or an isotype-matched control antibody (100 µg/mouse). Then, the mice were intranasally infected with H37Ra at a dose of 3.0×10<sup>5</sup> CFU/mouse in 100 µL PBS, followed by additional injections of neutralizing anti-IL-16 antibody three times weekly. After four weeks of infection, the mice were sacrificed to assess cytokine levels and bacterial load (Figure 8(b)). Treatment with the anti-IL-16 antibody reduced the levels of IL-16 in their BALF samples (Figure 8(c)) and prevented the survival of H37Ra in the lungs (Figure 8(d)), indicating that neutralization of IL-16 provides protection against mycobacterium infection. Surprisingly, BALF from mice treated with the anti-IL-16 antibody exhibited significantly lower levels of IL-10 and TGF-β compared to BALF from control-treated mice (Figure 8(e)). However, no changes in the levels of IL-6 and TNF-α were observed (Figure 8(f)). These results suggest that neutralization of IL-16 can effectively promote host clearance of Mycobacterium in vivo.

### **Discussion**

Here, we found that IL-16 was significantly increased in the serum of patients with active tuberculosis compared to patients with LTBI, so, IL-16 could be a potential biosignature for the diagnosis of TB. Then, we demonstrated that macrophages are a major resource of IL-16 secretion response to Mtb infection. Depending on the level of secretion after different mycobacterial infections, the amount of IL-16 may correlate with the virulence of mycobacteria. Additionally, we have revealed novel functions of IL-16 in facilitating Mtb intracellular survival by inhibiting phagosome maturation and repressing the expression of Rev-erba. In zebrafish larvae, inhibition of IL-16 resulted in less severe pathology and increased survival following *M. marinum* infection. Moreover, genetic deficiency of IL-16 enhanced bacterial clearance and reduced lung damage and pathology in mice challenged with Mtb. Furthermore, neutralizing IL-16 enhanced mycobacterium clearance in SCID mice. Thus, for the first time, we provide

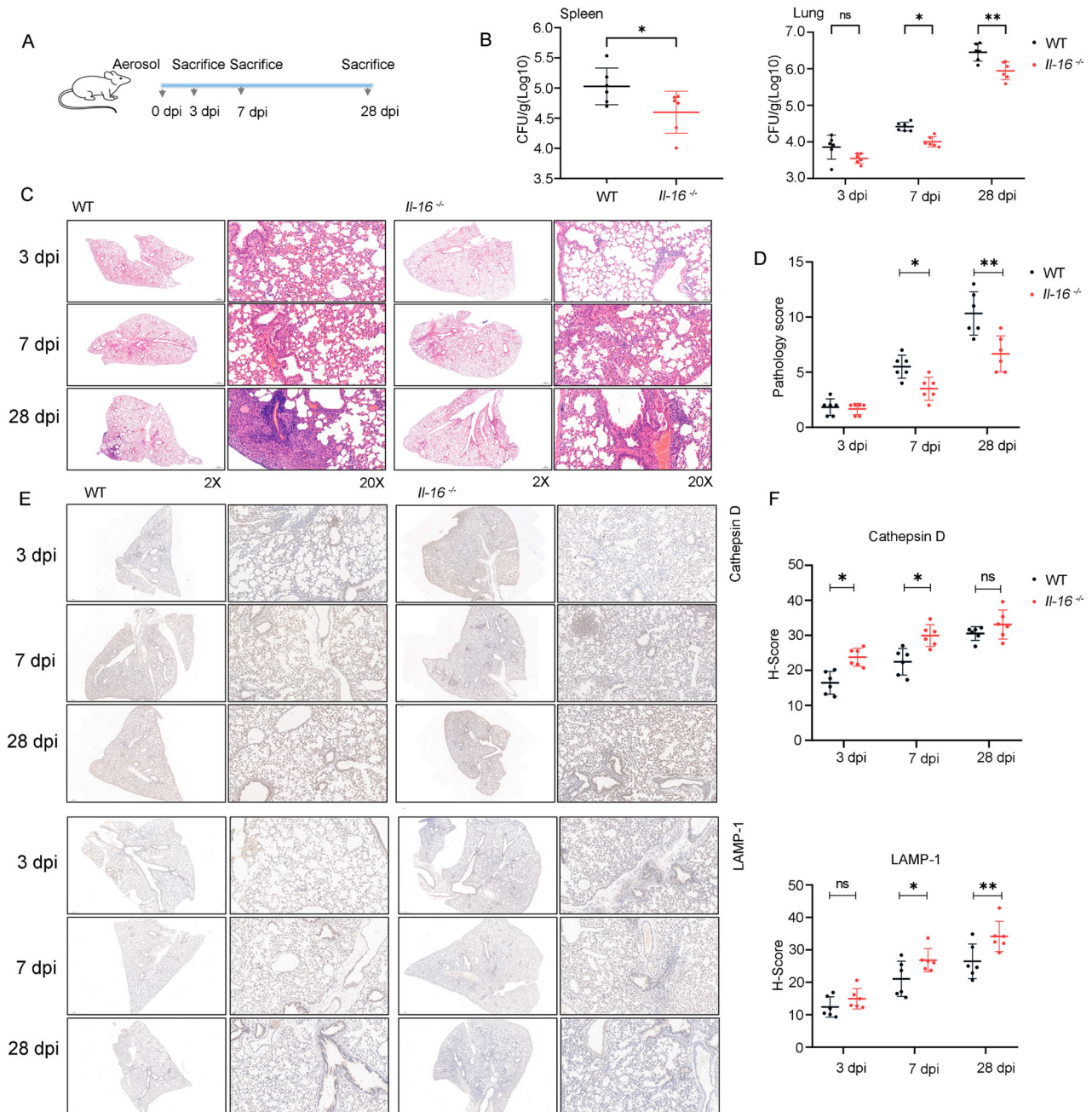


**Figure 7.** Interleukin 16 deficiency reduced the host susceptibility to H37Rv infection. **A** Schematic diagram of infection experiments. C57BL/6 or *Il-16*<sup>-/-</sup> mice were infected with ~200 CFU of H37Rv using a Glas-Col inhalation exposure system ( $n = 6$  to  $8$ ). **B** At 3-, 7- and 28-days post-infection, the mice were sacrificed, and bacterial counts in the lungs and spleens were determined on Middlebrook 7H10 agar. Mtb colonies were incubated at 37 °C and counted after 21 days ( $n = 6$ ). **C** For histopathology analysis, half of each lung was fixed in a 4% neutral-buffered paraformaldehyde solution for 24 hours. Lung tissue was then embedded in paraffin. A series of sections with a thickness of 4-7  $\mu$ m were then cut and stained with hematoxylin and eosin by standard methods. **D** Histopathology analysis was evaluated by pathologists in a blinded manner ( $n = 6$ ). **E** LAMP-1 and Cathepsin D expression were analyzed by immunohistochemistry. **F** H-Score analysis was determined according to **E**. The values are the means  $\pm$  SEM, 6 to 8 mice per group as indicated. \* $p < 0.05$  compared to media, Student's *t*-test.

evidence that IL-16 acts on host susceptibility response to Mtb infection, supporting IL-16 has the therapeutic value of anti-IL-16 antibodies in the treatment of TB.

IL-16 is a multifunctional cytokine initially characterized as a product of immunological competence cells such as lymphocytes and macrophages. Previous studies have identified various cell types as sources of secreted IL-16, including Thy1<sup>+</sup> T-cells, B220<sup>+</sup> B-cells,

CD4<sup>+</sup> and CD8<sup>+</sup> T-cells, and p46<sup>+</sup> NK-cells in type 1 diabetes [22]. Similarly, CD4<sup>+</sup> cells were identified as the main source of IL-16 during *Staphylococcus aureus* infection settings [24]. Here, we observed a reduction in IL-16 levels in the serum and BALF of H37Ra-infected mice with macrophage deletion, indicating that macrophages are likely the primary source of IL-16 production. IL-16 is initially transcribed as pro-IL-16, and its production is regulated at both

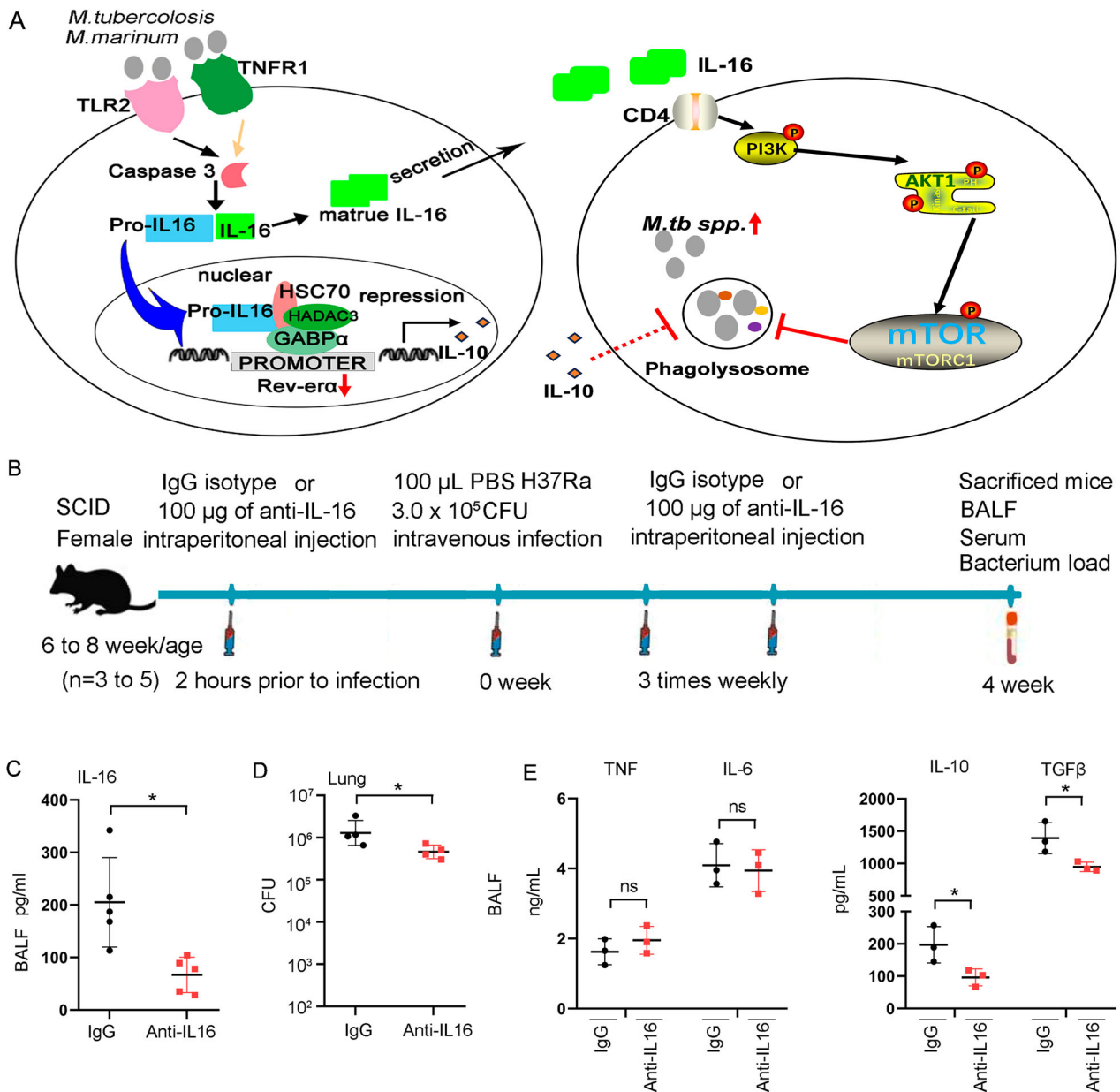


**Figure 8.** Neutralization of IL-16 contributes to host control of Mycobacterium infections. **A** Schematic diagram of GAPBA $\alpha$ /Pro-IL16/HDAC3 complex regulates Rev-erba expression and IL-16 regulates the maturation of phagolysosomes through CD4. **B** Schematic diagram of neutralization of IL-16 in vivo. 6-8 weeks of age mice were intraperitoneally injected with 200  $\mu$ g anti-IL-16 neutralizing mAb 2 h prior to infection. Mice were challenged with 3 $\times$ 10<sup>6</sup> CFU of H37Ra in 100  $\mu$ L PBS via the intravenous route, followed by intraperitoneal injection 3 times weekly with 200  $\mu$ g anti-IL-16 neutralizing mAb. Control mice received 200  $\mu$ g isotype-matched mouse IgG2a(k). The mice were sacrificed 4 weeks post-infection (n = 3 to 5). **C** IL-16 level in BALF by ELISA (n = 3 to 5). **D** H37Ra load in lung (n = 3 to 5). **E** TNF, IL-6, IL-10 and TGF- $\beta$  levels in BALF measured by ELISA (n = 3 to 5). \**p*<0.05 compared to media, Student's *t*-test. The graph shown is representative of 2 independent experiments.

the transcriptional level and through caspase-3-dependent processing [31]. In this context, the production of IL-16 to its active form is mediated by caspase-3 and caspase-8. When caspase-3/8 activity is blocked using inhibitors, the release of IL-16 is reduced. Furthermore, the TNF cascade plays a central role in inducing IL-16 processing in CD4<sup>+</sup> T cells, demonstrated by observing diminished IL-16 production in MRSA-infected mice lacking TNFR1 [24]. Additionally, TNFR1 blocking reduced the production of IL-16 after *M. marinum* infection in macrophages. Interestingly, treatment with TLR2 antibody also interferes

with the secretion of IL-16. Thus, IL-16 production appears to be specifically linked to TNFR1, TLR2 and other receptors, including EGFR and FasL, which were also found to be involved in initiating the processing of IL-16 to its active form. This requirement for multiple stimuli may also help explain why LPS alone or the tested Gram-negative airway pathogens were much less capable of stimulating IL-16 production.

IL-16 secretion has been implicated in various diseases, including atopic diseases and sarcoidosis granulomas [32]. Here, IL-16 was directly related to the activity

of the TB disease because the successful treatment of TB was associated with decreased circulating levels of IL-16, suggesting that elevated circulating IL-16 levels could be a consequence of Mtb infection. However, it is unclear whether endogenous production of IL-16 is essential for the replication of Mtb and the worsening of pathological conditions. In this study, we provide the first evidence that IL-16 secretion is likely critical for modulating TB pathology. We found that genetic deficiency of IL-16 in *Il-16<sup>-/-</sup>* mice resulted in enhanced clearance of bacteria and diminished lung pathology compared to WT mice. According to this finding and considering that macrophages are the most likely source of IL-16 in this setting, we hypothesized that macrophage-derived IL-16 contributes to TB progression. To investigate this hypothesis, we used zebrafish larvae infected with *M. marinum*, a close genetic relative of *M. tuberculosis* and the causative agent of TB in ectotherms. Zebrafish larvae have been reported to have immature T cells before 3 to 4 weeks post-fertilization, with their immune protection against bacterial infection mainly dependent on macrophages at 26 h post-fertilization [33]. This model has provided important insights into the pathogenesis and genetics of human TB through macrophage-mediated protection [34, 35]. We found that IL-16 morphants larvae had reduced bacteria burdens and decreased mortality of the embryos compared with WT larvae. Moreover, the neutralization of IL-16 enhanced *H37Ra* clearance in SCID mice, which were identified to be deficient in T leukomonocytes. Therefore, this is the first study to reveal that macrophage-derived IL-16 enhances host sensitivity to Mtb infection.

Our findings suggest that IL-16 plays a role in mediating its effects during Mtb infection. When IL-16 was neutralized, there was a down-regulation of IL-10 levels in the BALF of H37Ra-infected mice. IL-10 has been shown to interfere with the acquisition of microbicidal competence, suggesting that IL-16 may have the ability to directly inhibit pathogen clearance [29]. In this context, we observed that IL-16 deficiency resulted in reduced bacterial survival both in vitro and in vivo. IL-10 has also been previously demonstrated to attenuate the localization of mycobacteria within early phagosomes and to reduce the capacity of bacterium to traffic into a non-mature late phagosome [36]. In our results, *M. marinum* resided in late phagosomes, unable to fuse with lysosomes in rIL-16-treated macrophages. In contrast, genetic deficiency of IL-16 led to increased co-localization between H37Rv and phagolysosomes. These results indicated that IL-16 was likely related to the inhibited phagosome-lysosome fusion. However, whether IL-16 expression was associated with IL-10 secretion in response to Mtb infection remains unknown. Previously, the orphan nuclear receptor Rev-erba was shown to be essential for the clearance of mycobacterial infection

by inhibiting IL-10 production. In this study, we found that mycobacterium infection induced the translocation of Pro-IL16 into the nucleus, where it recruited GAPBA $\alpha$  and HDAC3 to repress Rev-erba expression. Based on these findings, we infer that IL-16 may repress Rev-erba expression, which in turn affects IL-10 expression, resulting in attenuated phagolysosome conversion and increased survival of bacteria under Mtb challenge conditions.

The role of IL-16 in various diseases and infection settings has been investigated. In the case of MRSA pneumonia, IL-16 has been shown to contribute to lung pathology [24], and treatment of pre-diabetic NOD mice with a neutralizing anti-IL-16 mAb beginning at the outset of mature IL-16 expression in islets provided optimum protection against destructive insulinitis and type 1 diabetes [37]. Administration of recombinant IL-16 exacerbates lung inflammation and associated pathology while reducing IL-16 expression through the delivery of a miR-125a mimic attenuates pristane-induced lung inflammation [38]. Here, we revealed that neutralizing endogenous IL-16 activity may have therapeutic value for treating TB based on our finding that neutralizing IL-16 reduces mycobacterial loads in the lungs of H37Ra-challenged mice. This suggests that targeting IL-16 could be a potential therapeutic strategy for TB treatment, considering the relationship between therapeutic targets and the stage of disease treatment recommended for TB. Furthermore, this concept of targeting IL-16 may have implications for other diseases associated with auto-inflammation- and infectious diseases.

In conclusion, our study highlights several important findings. First, we observed that IL-16 levels are specifically higher in active TB patients than those with LTBI, healthy donors, and the diagnostic potential of IL-16 for TB was indicated by ROC analysis. Second, we demonstrated that macrophages are a major source of IL-16 secretion in response to Mtb infection. Third, we found that IL-16 production promotes intracellular survival of Mtb by inhibiting phagosome maturation and repressing the expression of Rev-erba. Fourth, genetic deficiency of IL-16 enhanced bacterial clearance and reduced lung pathology in both Mtb-challenged mice and *M. marinum*-infected zebrafish larvae. Lastly, the neutralization of IL-16 enhanced pathogen clearance in H37Ra-infected SCID mice. Thus, these findings provide direct evidence of the contribution of IL-16 to host susceptibility in Mtb infection and suggest IL-16 as a promising target for treatment of TB.

## Materials and methods

### Study groups

Participants were selected based on Mtb-specific TSPOT responses, which are routinely performed to

diagnose Mtb infection at the Pulmonary Hospital of Tongji University. The diagnosis of tuberculosis was based on multiple criteria, including the TSPOT test, TB culture test, and sputum smear test, and recognized active TB when any two positives were met, which was reconfirmed based on imaging findings on lung CT. The participants were categorized into five groups: (1) active TB patients, (2) individuals with LTBI, (3) subjects with NTM infections, (4) patients with pulmonary tumours, and (5) healthy volunteers. The final diagnosis was made by a clinician who validated these criteria along with clinical symptoms. LTBI was diagnosed in individuals with a positive Mtb-specific TSPOT response but lacked clinical or radiographic evidence of active TB. NTM infected patients are patients infected with organisms other than *Mycobacterium tuberculosis*. Healthy control subjects were recruited if they had a negative Mtb-specific TSPOT response and no pulmonary symptoms or active disease.

Cohort 1 comprised 8 patients diagnosed with active TB, 5 patients with LTBI, and 5 healthy control subjects. Among them, 5 patients were undergoing antibiotherapy for 3 months. All patients and subjects were HIV-negative, not using immunosuppressive medications, had no clinical complications and were consecutively enrolled in the study (Details in Supplementary information Table 1 for cohort 1). Cohort 2 comprised 151 patients diagnosed as active TB (151 TSPOT positive, 137 smear positive and 132 TB culture positive), 31 patients with LTBI (31 TSPOT positive, 0 smear negative, 0 TB culture negative), 40 healthy control subjects, 112 NTM infection subjects, and 33 pulmonary tumour patients (Details in Supplementary information Table 2 for cohort 2). This study was approved by the Human ethical committee of Pulmonary Hospital of Tongji University (Shanghai, China; protocol no. K22-041Y in 2022).

### Animals

C57BL/6 and *Il-16*<sup>-/-</sup> were obtained from Shanghai Model Organisms (Shanghai, China). All mice were bred in specific pathogen-free conditions at the Laboratory Animal Center of Fudan University. Both female and male mice aged 6-8 weeks were used for the study. Ethical approval for the study was obtained from the ethical committee of Fudan University (Shanghai, China; protocol no. JS-016 in 2019).

### Cell culture

Peripheral blood mononuclear cells (PBMCs) were isolated from human blood using Ficoll-Paque (GE Healthcare, Chicago, IL, USA). Human monocyte-derived macrophages were purified by positive selection of CD14 and CD16 cells from the PBMCs using

MACS Microbeads from Miltenyi Biotec (Leiden, Netherlands), following the manufacturer's protocol. The isolated monocytes were then induced with 20 ng/mL of macrophage colony-stimulating factor (R&D Systems, Minneapolis, USA) in RPMI-1640 medium supplemented with 10% fetal bovine serum (STEMCELL Technologies), 100 U/mL of penicillin/streptomycin (Thermo Fisher Scientific), 10 mM Glutamax, and 10 mM pyruvate. Mouse alveolar macrophages (AMs) and bone marrow-derived macrophages (BMDMs) were isolated from control mice as previously describe [39, 40] and cultured in RPMI-1640 medium supplemented with 10% (v/v) fetal calf serum and 2 mM glutamine with penicillin (100 U/mL)/streptomycin (100 mg/mL) and M-CSF (10 ng/mL, Sino Biological, 51112-M08H). The cells were grown in 96-well plates (200 µL final volume; Corning Inc., Corning, NY, USA) and incubated at 37 °C in a humidified incubator with 5% CO<sub>2</sub>.

### Infection procedure in vitro

Macrophages/monocyte-derived macrophages were cultured at 37°C with 5% CO<sub>2</sub>. For infection experiments, cells were infected with mycobacteria at different bacterium-to-cell ratios (MOI = 1:1, MOI = 3:1, MOI = 5:1, or MOI = 10:1) for 4 h. After the infection, cells were washed to remove free bacteria and incubated in RPMI 1640 medium containing 10% fetal calf serum (FCS) [41, 42]. The cells were pretreated with neutralizing antibody anti-IL-16 (1 µg/ml, mouse IgG2a(κ) clone 14.1 #554734; BD Bioscience), rIL-16 protein (10 ng/ml, #ab256039 or #ab256040, Abcam) or not for 18 h. Following infection, neutralized anti-IL-16 antibodies or rIL-16 protein were added to the cell culture every other day. Cells were also pretreated with neutralizing antibodies or IgG isotype control 1 h prior to infection. The neutralizing antibodies used included anti-TLR4 (2 µg/mL; #AF1478; BD Biosciences), anti-TLR2 (2 µg/mL; mouse IgG2b Clone #383936; BD Biosciences), or anti-TNFR1 (2 µg/mL; mouse IgG1 Clone #16803; BD Biosciences). IgG isotype controls were used as a comparison at a concentration of 2 µg/mL (BD Biosciences). To assess the levels of IL-16 in the cell culture supernatants, respective inhibitors were added 1 h prior to infection, including caspase 3 inhibitor (C3 inh, 50 µM, Calbiochem), caspase-8 inhibitor (C8 inh, 50 µM, Calbiochem), and pan-caspase inhibitor (ZVAD, 100 Mm, Santa Cruz). Bacterial colony-forming units (CFUs) were determined by plating gradient dilutions of lysed cells onto 7H10 agar.

### Infection procedure in vivo

Clodronate liposomes or PBS control liposomes were obtained from ClodronateLiposomes.com (<http://>

www.clodronateliposomes.org/). To deplete lung macrophages, mice (6 to 8 weeks old) were administered intravenously with 150  $\mu\text{L}$  of clodronate liposomes or PBS control liposomes and intranasally with 50  $\mu\text{L}$  of clodronate liposomes or PBS control liposomes one day prior to mycobacterium infection [43]. Then, C57BL/6 mice were intravenously challenged with  $3.0 \times 10^6$  CFU of H37Ra in 100  $\mu\text{L}$  of PBS [44]. On the third day post-infection, mice (6 to 8 weeks old) were injected intranasally with 50  $\mu\text{L}$  of clodronate liposomes or PBS control liposomes [43, 45]. The mice were sacrificed 6 days post-infection to assess IL-16 levels in the BALF and serum.

*M. tuberculosis* H37Ra (ATCC 25177) and *M. tuberculosis* H37Rv (Pasteur strains) were grown, and suspensions were prepared as previously described [44, 46]. Briefly, Female C57BL/6 or SCID mice, aged 6 to 8 weeks, were intravenously challenged with  $1 \times 10^6$  CFU of *M. tuberculosis* H37Ra [44]. The mice were sacrificed 6 days post-infection to assay IL-16 level in BALF. Female C57BL/6 mice, aged 6 to 8 weeks, were intravenously challenged with  $1 \times 10^6$  CFU of H37Rv. At 4 or 12 weeks after infection, mice were sacrificed to determine IL-16 levels in BALF, serum, and lung homogenates. Lung homogenization was performed using an MM300 apparatus (Qiagen) and 2.5-mm diameter glass beads.

Mouse infection experiments were performed as previously described [47]. Briefly, C57BL/6 or *Il-16*<sup>-/-</sup> mice were infected with  $\sim 200$  CFU of H37Rv using a Glas-Col inhalation exposure system (Glas-Col Inc., Terre Haute, Ind.) [13]. At 3-, 7- and 28-days post-infection, the mice were sacrificed, and bacterial counts in the lungs and spleens were determined by plating 10-fold serial dilutions of individual organ homogenates on Middlebrook 7H10 agar supplemented with 10% Middlebrook OADC enrichment. *Mtb* colonies were incubated at 37 °C and were counted after 21 days. For histopathology analysis, half of each lung was fixed in a 4% neutral-buffered paraformaldehyde solution for 24 h. The lung tissue was embedded in paraffin, and sections with a thickness of 4-7  $\mu\text{m}$  were cut and stained with hematoxylin and eosin using standard methods. The pathology was evaluated by pathologists in a blinded manner [16].

### Neutralization of IL-16 in vivo

Mice aged 6-8 weeks were injected intraperitoneally with 200  $\mu\text{g}$  of anti-IL-16 neutralizing monoclonal antibody (#554734, clone 14.1, mouse IgG2a( $\kappa$ ); BD Bioscience) 2 h prior to infection. The mice were then challenged with  $3 \times 10^6$  CFU of H37Ra in 100  $\mu\text{L}$  of PBS via the intravenous route. After infection, the mice received intraperitoneal injections of 200  $\mu\text{g}$  of the 14.1 anti-IL-16 neutralizing monoclonal antibody thrice a week. Control mice were treated with

an isotype-matched mouse IgG2a( $\kappa$ ) antibody (#UPC 10, 200  $\mu\text{g}$ , Sigma). Four weeks post-infection, the mice were euthanized, and the levels of IL-16 in bronchoalveolar lavage fluid (BALF), H37Ra load in the lung, and cytokine levels in BALF were assessed.

### Zebrafish infection with *M. marinum*

The morpholino oligos of IL-16 MO (5'-AGAAT-GAGCTGGTTATTACCTGTGT-3') and con-MO (5'-CTACAGGTGAGCGGTATACAAGCTG-3', lowercase letters denote mismatched bases) were synthesized by Gene-Tools (LLC). The expression plasmid of *hIL-16* was purchased from BIO LTC company (Shanghai, China). IL-16 mRNA was transcribed in vitro using the Ambion® mMESAGE mMACCHINE® T7 Ultra Kit (Invitrogen, USA). For zebrafish experiments, 10 ng of IL-16 MO or con-MO and 100 pg of IL-16 mRNA were injected between 0 and 0.5 h post fertilization (h.p.f.) as previously described. The knockdown efficiency of IL-16 was assessed using qPCR with the following primers: Forward primer 5'-CGCTTCAGCTCATCCCCGTA-3'; Reverse primer 5'-CGGAGAACCCCTTTTAGCA-3'. Zebrafish embryos were incubated in FWPTU at 28°C to prevent pigment formation. Zebrafish infection with *M. marinum* was performed at 30 h.p.f., as previously described [34]. Briefly, Zebrafish larvae were infected by caudal vein injection with 1.0 to 1.5 nl per fish of a single-cell bacterial suspension in PBS at a concentration of  $5.0 \times 10^7$  CFU/mL. Bacterial burdens were assessed by plating the homogenates of fish livers onto 7H10 agar through serial dilution to determine the colony-forming units (CFU). For histopathological studies, larvae were sacrificed at the indicated times, fixed with 4% paraformaldehyde for 24 h and 70% ethanol for 24 h, and then prepared as paraffin blocks. Ziehl-Neelsen acid-fast staining (BA-409 TB stain kit; Baso, Zhuhai, China) was performed on 5  $\mu\text{m}$  sections for gross pathology according to the manufacturer's instructions. The sections were examined under an Olympus BH2 microscope (Tokyo, Japan), and images were captured using a digital camera (TK-C1481BEC; JVC, Tokyo, Japan). To assess bacterial burden via fluorescence microscopy, a half-area 96-well plate was prepared by adding 100  $\mu\text{L}$  of dH<sub>2</sub>O to the interwell space. Adding dH<sub>2</sub>O to the interwell space reduced evaporation within the wells and increased the thermal mass to lengthen the duration in which larvae remain cryo-anesthetized. Zebrafish larvae were then transferred to the plate, one larva per well, in 200  $\mu\text{L}$  of FWPTU (without tricaine), using a wide-bore P1000 pipette tip. To determine the analysis threshold, 3-5 uninfected larvae were included. The larvae were cryo-anesthetized by incubating the plate on ice for 10 min. Imaging was

performed using inverted x2 fluorescence microscopy, capturing images for further analysis.

### Statistical analysis

Statistical analysis was conducted using Prism (Graph-Pad Software). A two-tailed Student's *t*-test was used to compare two groups with a normal distribution. One-way analysis of variance (ANOVA) was used to analyze differences in means among multiple groups for continuous variables with a normal distribution. Survival curves were compared using the log-rank (Mantel–Cox) test. A significance level of  $P < 0.05$  was considered statistically significant for all analyses. Pearson's coefficient was used for correlation analysis. Data with three or more independent measurements are presented as mean  $\pm$  SEM.

### Disclosure statement

No potential conflict of interest was reported by the author (s).

### Funding

This work was supported by National Natural Science Foundation of China [grand number: 82271871, 81971900 and 82072245]; Grant from the major project of Study on Pathogenesis and Epidemic Prevention Technology System [grand number:2021YFC2302500]; Grant from the State Key Laboratory of Respiratory Disease, Guangdong-HongKong-Macao Joint Laboratory of Respiratory Infectious Disease [grand number: GHMJLRID-Z-202111]; National funded postdoctoral researcher program [grand number: GZC20230523]; Special Project of Guangdong Province Education Department in Key Fields [grand number: 2022ZDZX2050]; Basic and applied Basic Research of Guangzhou Science and Technology Bureau [grand number: 202201011717]; the open research funds from the Sixth Affiliated Hospital of Guangzhou Medical University, Qingyuan People's Hospital.

### Author contributions

WHZ and YX, resources; HBS, SFW, LLL, QS and YX, data curation; SFW, LLL, WJ and YX, software; HBS, LLL, WJ and YX, formal analysis; HBS, SFW, LLL, YTL, HXM and YMH, validation; SFW, LLL, YTL, HXM, WJ and YMH, investigation; HBS, WHZ, QS and YX, visualization; HBS, WJ, SFW, LLL, HHW and YX, methodology; HBS and YX, writing of the original draft; HBS, WHZ and YX, writing the review and editing; HBS, HHW, WHZ and YX, funding acquisition; HHW, WHZ and YX, project administration; HBS and YX, conceptualization; HBS, HHW, WHZ and YX, supervision. The order among co-first authors is determined by their contribution to performing experiments and writing the manuscript.

### Data availability statement

All data generated or analyzed during this study are included in this article and its supplementary information files. Further inquiries can be directed to the corresponding author.

### Materials availability

This study did not generate new unique reagents.

### References

- [1] Chakaya J, Khan M, Ntoumi F, et al. Global Tuberculosis Report 2020 - Reflections on the Global TB burden, treatment and prevention efforts. *Int J Infect Dis.* 2021;113(Suppl 1):S7–s12.
- [2] Wang L, Liu Z, Wang J, et al. Oxidization of TGF $\beta$ -activated kinase by MPT53 is required for immunity to *Mycobacterium tuberculosis*. *Nat Microbiol.* 2019;4(8):1378–1388.
- [3] Chakaya J, Petersen E, Nantanda R, et al. The WHO Global Tuberculosis 2021 Report - not so good news and turning the tide back to End TB. *Int J Infect Dis.* 2022;124(Suppl 1):S26–Ss9.
- [4] Carabalí-Isajar ML, Rodríguez-Bejarano OH, Amado T, et al. Clinical manifestations and immune response to tuberculosis. *World J Microbiol Biotechnol.* 2023;39(8):206.
- [5] Churchyard GJ, Kaplan G, Fallows D, et al. Advances in immunotherapy for tuberculosis treatment. *Clin Chest Med.* 2009;30(4):769–782, ix.
- [6] Mi J, Liang Y, Liang J, et al. The Research Progress in Immunotherapy of Tuberculosis. *Front Cell Infect Microbiol.* 2021;11:763591.
- [7] Bouzeyen R, Javid B. Therapeutic Vaccines for Tuberculosis: An Overview. *Front Immunol.* 2022;13:878471.
- [8] Uhlin M, Andersson J, Zumla A, et al. Adjunct immunotherapies for tuberculosis. *J Infect Dis.* 2012;205(Suppl 2):S325–S334.
- [9] Chai Q, Wang L, Liu CH, et al. New insights into the evasion of host innate immunity by *Mycobacterium tuberculosis*. *Cell Mol Immunol.* 2020;17(9):901–913.
- [10] Qiang L, Zhang Y, Lei Z, et al. A mycobacterial effector promotes ferroptosis-dependent pathogenicity and dissemination. *Nat Commun.* 2023;14(1):1430.
- [11] Hu Y, Wen Z, Liu S, et al. Ibrutinib suppresses intracellular mycobacterium tuberculosis growth by inducing macrophage autophagy. *J Infect.* 2020;80(6):e19–e26.
- [12] Chai Q, Lu Z, Liu CH. Host defense mechanisms against *Mycobacterium tuberculosis*. *Cell Mol Life Sci.* 2020;77(10):1859–1878.
- [13] Dai Y, Zhu C, Xiao W, et al. *Mycobacterium tuberculosis* hijacks host TRIM21- and NCOA4-dependent ferritinophagy to enhance intracellular growth. *J Clin Invest.* 2023;133(8).
- [14] Cohen SB, Gern BH, Urdahl KB. The Tuberculous Granuloma and Preexisting Immunity. *Annu Rev Immunol.* 2022;40:589–614.
- [15] Liu F, Chen J, Wang P, et al. MicroRNA-27a controls the intracellular survival of *Mycobacterium tuberculosis* by regulating calcium-associated autophagy. *Nat Commun.* 2018;9(1):4295.

- [16] Chai Q, Wang X, Qiang L, et al. A Mycobacterium tuberculosis surface protein recruits ubiquitin to trigger host xenophagy. *Nat Commun.* 2019;10(1):1973.
- [17] Wang J, Li BX, Ge PP, et al. Mycobacterium tuberculosis suppresses innate immunity by coopting the host ubiquitin system. *Nat Immunol.* 2015;16(3):237–245.
- [18] Herrera M, Keynan Y, Lopez L, et al. Cytokine/chemokine profiles in people with recent infection by Mycobacterium tuberculosis. *Front Immunol.* 2023;14:1129398.
- [19] Harris J, Hope JC, Keane J. Tumor necrosis factor blockers influence macrophage responses to Mycobacterium tuberculosis. *J Infect Dis.* 2008;198(12):1842–1850.
- [20] Bobadilla K, Jaime SE, González ME, et al. Human phagosome processing of Mycobacterium tuberculosis antigens is modulated by interferon- $\gamma$  and interleukin-10. *Immunology.* 2013;138(1):34–46.
- [21] Bai W, Liu H, Ji Q, et al. TLR3 regulates mycobacterial RNA-induced IL-10 production through the PI3 K/AKT signaling pathway. *Cell Signal.* 2014;26(5):942–950.
- [22] Cruikshank WW, Kornfeld H, Center DM. Interleukin-16. *J Leukoc Biol.* 2000;67(6):757–766.
- [23] Gorvel L, Al Moussawi K, Ghigo E, et al. Tropheryma whipplei, the Whipple's disease bacillus, induces macrophage apoptosis through the extrinsic pathway. *Cell Death Dis.* 2010;1(4):e34.
- [24] Ahn DS, Parker D, Planet PJ, et al. Secretion of IL-16 through TNFR1 and calpain-caspase signaling contributes to MRSA pneumonia. *Mucosal Immunol.* 2014;7(6):1366–1374.
- [25] Awuh JA, Flo TH. Molecular basis of mycobacterial survival in macrophages. *Cell Mol Life Sci.* 2017;74(9):1625–1648.
- [26] Liang M, Habib Z, Sakamoto K, et al. Mycobacteria and Autophagy: Many Questions and Few Answers. *Curr Issues Mol Biol.* 2017;21:63–72.
- [27] Miller BK, Hughes R, Ligon LS, et al. Mycobacterium tuberculosis SatS is a chaperone for the SecA2 protein export pathway. *Elife.* 2019; 8:e40063.
- [28] Zhang QA, Ma S, Li P, et al. The dynamics of Mycobacterium tuberculosis phagosome and the fate of infection. *Cell Signal.* 2023;108:110715.
- [29] Chandra V, Mahajan S, Saini A, et al. Human IL10 gene repression by Rev-erba ameliorates Mycobacterium tuberculosis clearance. *J Biol Chem.* 2013;288(15):10692–10702.
- [30] Zhang Y, Tuzova M, Xiao ZX, et al. Pro-IL-16 recruits histone deacetylase 3 to the Skp2 core promoter through interaction with transcription factor GABP. *J Immunol.* 2008;180(1):402–408.
- [31] Zhang Y, Center DM, Wu DM, et al. Processing and activation of pro-interleukin-16 by caspase-3. *J Biol Chem.* 1998;273(2):1144–1149.
- [32] Fava A, Rao DA, Mohan C, et al. Urine Proteomics and Renal Single-Cell Transcriptomics Implicate Interleukin-16 in Lupus Nephritis. *Arthritis Rheumatol.* 2022;74(5):829–839.
- [33] Xie Y, Meijer AH, Schaaf MJM. Modeling Inflammation in Zebrafish for the Development of Anti-inflammatory Drugs. *Front Cell Dev Biol.* 2020;8:620984.
- [34] Takaki K, Davis JM, Winglee K, et al. Evaluation of the pathogenesis and treatment of Mycobacterium marinum infection in zebrafish. *Nat Protoc.* 2013;8(6):1114–1124.
- [35] Lin C, Tang Y, Wang Y, et al. WhiB4 Is Required for the Reactivation of Persistent Infection of Mycobacterium marinum in Zebrafish. *Microbiol Spectr.* 2022;10(2):e0044321.
- [36] Mege JL, Meghari S, Honstetter A, et al. The two faces of interleukin 10 in human infectious diseases. *Lancet Infect Dis.* 2006;6(9):557–569.
- [37] Meagher C, Beilke J, Arreaza G, et al. Neutralization of interleukin-16 protects nonobese diabetic mice from autoimmune type 1 diabetes by a CCL4-dependent mechanism. *Diabetes.* 2010;59(11):2862–2871.
- [38] Smith S, Wu PW, Seo JJ, et al. IL-16/miR-125a axis controls neutrophil recruitment in pristane-induced lung inflammation. *JCI Insight.* 2018;3(15):e120798.
- [39] Cohen SB, Gern BH, Delahaye JL, et al. Alveolar Macrophages Provide an Early Mycobacterium tuberculosis Niche and Initiate Dissemination. *Cell Host Microbe.* 2018;24(3):439–46.e4.
- [40] Khan N, Mendonca L, Dhariwal A, et al. Intestinal dysbiosis compromises alveolar macrophage immunity to Mycobacterium tuberculosis. *Mucosal Immunol.* 2019;12(3):772–783.
- [41] Zhang G, Liu X, Wang W, et al. Down-regulation of miR-20a-5p triggers cell apoptosis to facilitate mycobacterial clearance through targeting JNK2 in human macrophages. *Cell Cycle.* 2016;15(18):2527–2538.
- [42] Hill NS, Welch MD. A glycine-rich PE\_PGRS protein governs mycobacterial actin-based motility. *Nat Commun.* 2022;13(1):3608.
- [43] Jackson MV, Morrison TJ, Doherty DF, et al. Mitochondrial Transfer via Tunneling Nanotubes is an Important Mechanism by Which Mesenchymal Stem Cells Enhance Macrophage Phagocytosis in the In Vitro and In Vivo Models of ARDS. *Stem Cells.* 2016;34(8):2210–2223.
- [44] Frigui W, Bottai D, Majlessi L, et al. Control of M. tuberculosis ESAT-6 secretion and specific T cell recognition by PhoP. *PLoS Pathog.* 2008;4(2):e33.
- [45] Alikhanyan K, Chen Y, Kraut S, et al. Targeting alveolar macrophages shows better treatment response than deletion of interstitial macrophages in EGFR mutant lung adenocarcinoma. *Immun Inflamm Dis.* 2020;8(2):181–187.
- [46] Wu X, Wu Y, Zheng R, et al. Sensing of mycobacterial arabinogalactan by galectin-9 exacerbates mycobacterial infection. *EMBO Rep.* 2021;22(7):e51678.
- [47] Yang Q, Liao M, Wang W, et al. CD157 Confers Host Resistance to Mycobacterium tuberculosis via TLR2-CD157-PKCzeta-Induced Reactive Oxygen Species Production. *mBio.* 2019;10(4):e01949-19.